An Automatic and Accurate Localization System for Firefighters

Jinyang Li*, Zhiheng Xie†, Xiaoshan Sun*, Jian Tang*, Hengchang Liu* and John Stankovic†
*School of Computer Science and Technology
University of Science and Technology of China, Anhui, China
Email: {ljyustc, sxs1166, sa514015}@mail.ustc.edu.cn, hcliu@ustc.edu.cn
†Department of Computer Science
University of Virginia, Charlottesville, VA 22903, USA
Email: {zx3n, stankovic}@virginia.edu

***Abstract*—Firefighters' safety is a critical problem and a major issue is the lack of reliable indoor firefighter localization. State of the art approaches have failed to provide an automatic, accurate and reliable solution to localize firefighters in harsh environments. This paper presents a novel system to achieve this goal, by combining pedestrian dead reckoning with a recently emerging breadcrumb system. Our solution includes a new collaborative localization algorithm that contains a novel marginalization scheme and can improve the location accuracy of firefighters. We fully implement the algorithm in a complete system and conduct experiments in both an office building and in a simulated firefighting scene that involved a real fire and professional firefighters. Evaluation results from a 400 meter-long trace demonstrate that our approach significantly reduces the average and maximum firefighter location error to 1.4% and 2.7% of the total distance, respectively.**

***Keywords*-Breadcrumb system; indoor localization; relative measurement graph;**

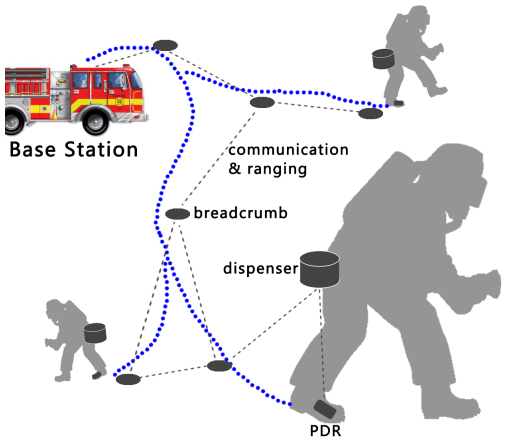

Figure 1. System overview.

I. Introduction

Our society relies on a multitude of public safety personnel, e.g., firefighters. While firefighters protect our lives in many respects, they often place themselves in danger when dealing with fires. The September 11 attacks in New York killed 343 American firefighters [1]. If we could know the accurate locations of firefighters in real time, it would help incident commanders to warn them of invisible dangers ahead, and may even allow injured firefighters to be rescued. While previous work has taken initial steps towards this goal, in practice it is still limited to vocal reports which requires the involvement of firefighters [2]. The communication quality is another critical issue [3], and some solutions also suffer from long setup time (typically 1-2 hours) while establishing new base stations as anchor nodes [4]. Other solutions rely on floor plans or other environmental information to minimize the error accumulation of using a Pedestrian Dead Reckoning (PDR) approach [5].

The specific characteristics of the indoor localization problem in a firefighting scenario consist of two aspects. First, harsh and complicated environments add practical constraints: (1) there usually is no reliable power supply in the building during the fire, (2) there is low ambient light, (3) smoke and (4) heat. Second, compared to consumer-oriented applications, rescue tasks have unique requirements: (1) energy is not a main concern; (2) firefighters have to carry professional equipment, such as an air respirator, fire hose and axe and other equipment; (3) they have to focus on rescue tasks; and (4) their locations need to be accessible to themselves and their on-site commanders outside the building. A more detailed analysis of requirements and system architecture consideration for first responder systems can be found in [6]. Imagine, however, that we have a quickly deployable on-site wireless sensor network (WSN) that is able to connect firefighters to outside incident commanders and help localize firefighters. Such a system has the potential to overcome the difficulties above.

But how can we deliver such a real time WSN-assisted indoor localization system? Most existing generalized localization methods only address part of the problem. For example, most infrastructure-based methods [7]–[9] assume that sensor nodes have been pre-installed or need to be manually deployed before they are used for localization. The challenge is that pre-deployed sensor nodes are probably not working any more due to fire, explosion, collapsed walls, and so forth [3]; what may also not be working are the WiFi and cellular stations in the building [10]. Solutions where

firefighters manually deploy sensor nodes distract them from their primary fire fighting and rescue work and hamper their safety as well.

In recent years, a promising solution called the breadcrumb system [10]–[12] was proposed to transmit users' physiological parameters that measure life critical functions to an incident commander reliably in real time. Each firefighter carries multiple breadcrumbs (sensor nodes) in his breadcrumb dispenser and a breadcrumb is automatically deployed whenever a communication connection to the breadcrumb chain gets weak, establishing a dynamically emerging wireless sensor network. Breadcrumbs are deployed as a firefighter enters so they are not burned up ahead of time. If they get burned up later then new ones are automatically dropped as firefighters walk around. Motivated by this recent development, we create a solution to achieve an automatic and accurate indoor localization system and reliable communication system at the same time by combining a breadcrumb system, a conventional PDR approach, and a new localization algorithm. Firefighters are passive with respect to localization, thus the system does not affect their primary tasks. A system overview is shown in Fig. 1.

The main contributions of this paper include:

- A new collaborative localization algorithm is created that is efficient and can run in real-time. It permits incremental updates to location estimates and provides error estimations. Its solution leverages measurements from a breadcrumb system and a PDR system.
- The localization algorithm is fully implemented and integrated into a complete real-time indoor localization system that does not require firefighters' involvement.
- To the best of our knowledge, we provide the first experiment on communication and localization using a breadcrumb system where real fire, smoke and professional firefighters are used.
- One evaluation of the system is from indoor traces of 400 meters. The results demonstrate that our approach reduces the average firefighter location error to 5.6 meters and the maximum error to 10.9 meters, which implies a promising error factor of only 1.4% and 2.7% of total distance. These results outperform a baseline based solely on PDR. Overall, the evaluation results show that our solution successfully achieves region-level accuracy and is robust in complicated real-world indoor environments.

The remainder of this paper is organized as follows. We compare our work with the state of the art in Section II. Then an overview of the system design is presented in Section III. The collaborative localization method is described in Section IV. The implementation and evaluation results are shown in Section V. Finally, we conclude the paper in Section VI.

II. Related Work

Localizing firefighters is challenging when they are in large commercial buildings or complicated industrial buildings that generally aren't accommodating to standard GPS technology. The current standard approach for firefighter localization is based on vocal communication. In fact, vocal communication is used in almost all first response applications via standard communication devices like P25 systems [2]. Firefighters report their approximate positions to the incident commander periodically, sometimes with positions stated as stairways or near particular windows. This method is highly problematic due to the chaotic environment. To make it worse, the communication is often lost when firefighters go to higher floors or enter basements [3], and subsequently firefighters can no longer be localized.

The Department of Homeland Security is seeking for techniques to assist indoor firefighter localization. For instance, WPI proposed to use fire trucks as temporary base stations when the firefighters arrive at the site and adopt the traditional triangulation approach, but this method suffers from a long setup time of between one to two hours [4]. Honeywell proposed to use foot-mounted sensors to collect step data and estimate the position of firefighters. However, the accuracy of the approach is unsatisfactory since firefighters change their step distances in different environments and errors accumulate. Furthermore, the localization process fails when communication is interrupted.

Academic and industry research has taken important steps towards accurate indoor localization using various approaches which can be classified into two classes: infrastructure-based and infrastructure-free. The first class utilizes WiFi, lights or other pre-installed devices to localize users. For example, [13] proposed a WiFi based localization system using Synthetic Aperture Radar (SAR) to emulate large antenna arrays on commodity mobile device. The device can be located with a median error of 39 cm in three dimensional space. [14] presented a solution based on visible light. They use polarization to encode location information of light sources, so that flicking can be avoided. However, pre-installed infrastructure would probably not work any more due to fire, explosion, collapsed walls, and so forth [3].

The second category does not require pre-installed indoor infrastructure. For instance, the No.1 rank of 2015 Microsoft Indoor Localization competition [15] achieved 20 cm localization accuracy using a HDL-32E high definition LIDAR with typical accuracy of 2 cm [16]. Although accurate, LIDAR devices are too expensive and suffer performance degradation in smoky environments. Similarly, ultrasonic-based and depth-perception-based techniques may face the problem that the environment's temperature exceeds sensor's operating range. The change rate of speed of sound is approximately $1\%/5.7^{\circ}C$. Affected by the heat and temper-

ature variation in the on-fire building, readings of ultrasonic ranging become less reliable in the non-homogeneous environment.

Researchers have also explored using the Pedestrian dead reckoning (PDR) for firefighter localization. However, it is well known that PDR suffers from error accumulation and cannot achieve long term accuracy. To cope with this problem, it is natural to calibrate the result of PDR with some form of landmarks. For instance, [17] shows a promising civilian unsupervised indoor localization solution that combines dead reckoning with landmarks naturally existing in buildings identified by signatures on multiple sensing dimensions. [5] describes how to combine PDR with the floor plan to eliminate the location error. However, as mentioned before, all types of pre-installed devices cannot guarantee their availability when the building is on-fire. Moreover, we argue that it is not reasonable to assume that the floor plan, especially an up-to-date floor plan, is available for each building.

More recently, a breadcrumb system has been proposed to help improve the communication between firefighters and incident commanders. The National Institute of Standard and Technology first proposed the use of dynamically dropping sensor nodes to form a relay network [3], and [10] provides the first systematic design for breadcrumb systems with extensive real-world experiments. Then a series of related problems have been addressed, such as optimized collaboration strategy for multiple firefighters [11], delay tolerant networking (DTN) when all firefighters run out of breadcrumbs [18], and handling the body shadowing effect in narrow spaces [12]. However, to the best of our knowledge, so far there is not yet a holistic solution for firefighter localization using a breadcrumb system.

We also note that there have been work on combining PDR with wireless sensor networks (WSN) [7]–[9]. For example, [7] proposed a WSN-aided PDR solution with a hip-mounted IMU. The Euclidean distance measurements to anchor nodes are fused with PDR outputs through an extended Kalman filter. However, all these existing works assume that the location of sensor nodes are fixed and the topology of the sensor network is unchanged. But in our system, breadcrumbs themselves are deployed automatically from a dispenser with only estimated positions. In addition, the topology of breadcrumb chains is dynamically changed. Breadcrumbs may be burned up, destroyed by a collapsed wall, kicked by firefighters in the darkness, etc. As a result, adding, removing and moving breadcrumbs are frequent. These factors no doubt make the problem much more challenging.

III. System Design

We present the design details of our proposed system in this section. The ultimate goal is to localize firefighters in an unfamiliar building with region-level accuracy. In our system, each firefighter is equipped with a foot-mounted PDR unit and carries *breadcrumbs* in the *dispenser*. The PDR unit is to estimate the displacement as a firefighter moves. The breadcrumb system is used to relay data and also provide relative distance measurements among system nodes (breadcrumbs and firefighters). By collecting all these position related measurements, a collaborative localization algorithm is applied, which gives the position estimations for both firefighters and breadcrumbs.

A PDR consists of an accelerometer and a gyroscope, which keeps track of the acceleration and angle velocity over time. By using inertial dynamic equations combining with the zero-velocity update error correction [19], [20], the PDR outputs a firefighter's displacement estimation between any two time points.

As firefighters move, breadcrumbs are dropped on the ground, generating a chain to relay data from firefighters to the base station outside the building. The data could be firefighters' vital signs, voices, pictures or location information. Meanwhile, a breadcrumb estimates the relative distance between itself and another system node (another breadcrumb or a dispenser) by using the receive signal strength indicator (RSSI).

By collecting all these relative position related measurements through the breadcrumb chain to the base station, a relative measurement graph (RMG) is built, where breadcrumbs as well as firefighters are nodes, and measurements are the edges. Then a novel *collaborative localization algorithm* is applied to the RMG to estimate the positions of firefighters and breadcrumbs. The algorithm is highly scalable, which allows nodes to join and leave the graph dynamically. This is because once a change occurs, only related nodes' positioning information needs to be updated.

Firefighters always work in groups for rescuing or putting out the fire. The analysis and model of incident scene mobility can be found in [21] and [22]. It is forbidden to act alone, especially in poor visibility area. When in the on-fire building, firefighters rely on breathing apparatus to breath. Generally, a fully filled oxygen tank provides about 20 to 30 minutes of air supply (depending on the firefighter's physique and activity intensity). If the task last hours, firefighters would need to retreat and replace their oxygen tanks. After the fire, firefighters also need to check the burned plots for several times to prevent rekindle. Therefore, firefighters will go through the same place several times. Our previous works have addressed the coordinated deployment problem to achieve efficient and balanced deployment scheme in a group of firefighters [10], [11]. [23] studied the relay placement problem in polymorphous network which is also related to the deployment scheme. In this work, we focus on the collaborative localization problem when using breadcrumb systems.

A key factor that boosts our system is to leverage the position *correlation* between firefighters and breadcrumbs. On

one side, breadcrumbs can be used to "calibrate" firefighters' position estimation. On the other side, a firefighter can strengthen the position correlation between two breadcrumbs by new measurements provided by the PDR when the firefighter goes from one breadcrumb to the other.

IV. Collaborative Localization

We describe the collaborative localization algorithm in this section. A *relative measurement graph* (RMG) is defined as $G = (V, E, F)$, where V is the vertex set, including all interested nodes to be localized; E is the edge set, representing the measurement relationship between nodes; and F is the mapping $E \to (Z, P)$, where Z is the set of all the measurements and P is the set of the error (noise) covariance matrices of the measurements. Assume there are totally n nodes in a breadcrumb network, Node i's location is $\mathbf{x}_i = [x_i, y_i, z_i]^T (i = 1, \cdots, n)$.

The position of the base station is assumed to be known (obtained via GPS). There are two types of measurement in breadcrumb system: the relative position measurement and the relative range measurement. PDR units provide relative position measurements. Consider a moving firefighter who drops two consecutive breadcrumbs i and j. Let ζ_{ij} denote the noisy relative position measurement given by the PDR unit, and ωij is the measurement noise. Then the relative position measurement between i and j is modeled as

$$\zeta_{ij} = \mathbf{x}_i - \mathbf{x}_j + \omega_{ij}$$

The other measurement is a relative range measurement. In the breadcrumb system, the relative range between two nodes is estimated by the RSSI distance estimator. Let r_{ij} denote the relative range measurement and γij the measurement noise between Node i and Node j, then the relative range measurement is modeled as

$$r_{ij} = \|\mathbf{x}_i - \mathbf{x}_j\| + \gamma_{ij}$$

All the above measurements can be written in a uniform formula as

$$\mathbf{z}_{ij} = h(\mathbf{x}_i, \mathbf{x}_j) + \epsilon_{ij} \tag{1}$$

where $\mathbf{z}_{ij}$ is the noisy measurement, ϵ_{ij} is the measurement noise, and $h(\cdot)$ is the measurement function. For binary relative position measurement, $h(\mathbf{x}_i, \mathbf{x}_j) = \mathbf{x}_i - \mathbf{x}_j + \epsilon_{ij}$. For binary relative range measurement, $h(\mathbf{x}_i, \mathbf{x}_j) = \|\mathbf{x}_i - \mathbf{x}_j\| + \epsilon_{ij}$.

A. Estimation on Relative Measurement Graph

The estimation problem on RMG with linear measurements is discussed in [24], [25]. Assume there are m relative position measurements about the n nodes in the breadcrumb network, denoted as $\zeta_{ij} = \mathbf{x}_i - \mathbf{x}_j + \epsilon_{ij} \in \mathbb{R}^3, (i, j \in \{1, \cdots, n\})$, where $\epsilon_{ij} \in \mathbb{R}^3$ is the random error vector with zero mean. Let $\mathbf{x}$ denote all the positions of the n nodes $\mathbf{x} = [\mathbf{x}_1^T, \mathbf{x}_2^T, \cdots, \mathbf{x}_n^T]^T \in \mathbb{R}^{3n}$, $\mathbf{z}$ denote all the noisy measurements $\mathbf{z} = [\zeta_1^T, \zeta_2^T, \cdots, \zeta_m^T]^T \in \mathbb{R}^{3m}$, and ϵ denote the measurement noises $\epsilon = [\epsilon_1^T, \epsilon_2^T, \cdots, \epsilon_m^T]^T \in \mathbb{R}^{3m}$. The uncertainty of a measurement is represented by a covariance matrix $\mathbf{P}_k = \mathbb{E}[\epsilon_k \epsilon_k^T] \in \mathbb{R}^{3\times 3}, (k = 0, \cdots, m)$. Then the measurement equation can be written as

$$\mathbf{z} = \mathcal{A}^T \mathbf{x} + \epsilon \tag{2}$$

where $\mathcal{A} = \mathbf{A} \otimes \mathbf{I}$, $\mathbf{A}$ is the incidence matrix of the measurement graph G, $\mathbf{I}$ is the 3×3 identity matrix, and $\otimes$ denotes the Kronecker product.

An example of one base station and three breadcrumbs is shown in Fig. 4. The solid red circle represents the base station whose position is known. The hollow black circles represent deployed breadcrumbs. The edges are the relative position measurements. The measurement noises are annotated on the corresponding edges. The corresponding equation is listed below the graph. The incidence matrix $\mathbf{A}$ of graph G is a $n \times m$ matrix, where one row corresponds to one node and one column corresponds to one edge, which indicates if a node is involved in an edge (measurement) and what the direction it is. For example, edge e_4 (measurement ζ_4) involves Node 2 and Node 3, and the direction is from Node 2 to Node 3. This corresponds to $\mathbf{A}_{24} = \mathbf{I}$ and $\mathbf{A}_{34} = -\mathbf{I}$.

The position vector $\mathbf{x}$ can be partitioned into an anchor node variable vector $\mathbf{x}_r$ (in the example, the position of the base station) and a non-anchor node variable vector $\mathbf{x}_b$ (in the example, the positions of the 3 deployed breadcrumbs). The incidence matrix can also be partitioned to an anchor node matrix $\mathbf{A}_r$ and a non-anchor node matrix $\mathbf{A}_b$. Then (2) can be rewritten as

$$\bar{\mathbf{z}} = \mathcal{A}_b^T \mathbf{x}_b + \epsilon \tag{3}$$

where $\bar{\mathbf{z}} = \mathbf{z} - \mathcal{A}_r^T \mathbf{x}_r$. Obtaining an estimate of $\mathbf{x}_b$ becomes a classical estimation problem, which can be solved by *Best Linear Unbiased Estimator* (BLUE) [26]. The best estimate of $\mathbf{x}_b$ in the linear combination space of all the measurements is uniquely determined by $\hat{\mathbf{x}}_b$ in the following linear system

$$\mathcal{L}\hat{\mathbf{x}}_b = \mathbf{b} \tag{4}$$

where $\mathcal{L} = \mathcal{A}_b \mathcal{P}^{-1} \mathcal{A}_b^T$ is called G's *Kirchhoff Matrix*, $\mathbf{b} = \mathcal{A}_b \mathcal{P}^{-1} \bar{\mathbf{z}}$ and $\mathcal{P}$ is a block diagonal matrix consisting of all the covariance matrices $\mathbf{P}_k$ of $\epsilon_k, (k = 1, \cdots, m)$. BLUE has the smallest variance for the estimation error $\mathbf{x}_b - \hat{\mathbf{x}}_b$ among all linear estimators [26]. The covariance matrix of the estimation errors is given by

$$\mathbf{\Sigma} = \mathbb{E}[(\mathbf{x}_b - \hat{\mathbf{x}}_b)(\mathbf{x}_b - \hat{\mathbf{x}}_b)^T] = \mathcal{L}^{-1} \tag{5}$$

However, BLUE has several disadvantages when being applied to the breadcrumb system. First, the computation complexity of BLUE is very high. Assuming there are n nodes, m measurements, and a constant number of anchors in the network, the computational complexity for $\mathbf{\Sigma}$ is

Figure 2. The hardware prototype.

Figure 3. Breadcrumb system in action.

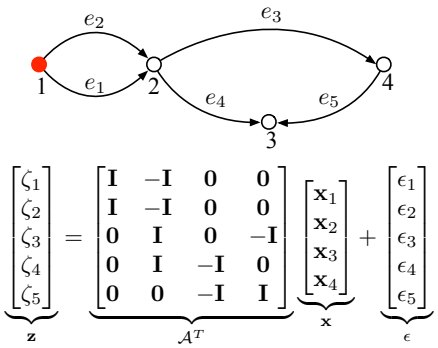

Figure 4. An RMG example.

$T(\mathbf{\Sigma}) = O(n^2m)$ since $T(\mathcal{L}) = T(\mathcal{P}^{-1}) + T(\mathcal{A}_b\mathcal{P}^{-1}) + T((\mathcal{A}_b\mathcal{P}^{-1})\mathcal{A}_b^T) = m + nm + n^2m = O(n^2m)$ and $T(\mathcal{L}^{-1}) = n^3$. And the complexity for calculating the estimation is $T(\hat{\mathbf{x}}_b) = O(n^2m)$ since $T(\hat{\mathbf{x}}_b) = T(\mathcal{L}^{-1}) + T(\mathbf{b}) + T(\mathcal{L}^{-1}\mathbf{b}) = (m + nm + n^2m + n^3) + nm + n^2 = O(n^2m)$. The solution does not scale since the computational complexity depends on the measurements number m which is very large in practice ($m \gg n$). Second, BLUE follows a one-time calculation scheme. When the measurement graph is changed, all previous calculations need to be re-executed. Such changes include new generated measurements and nodes leaving or joining the network, which are common in the breadcrumb system. Third, there are relative ranging measurements, which are non-linear, in the breadcrumb network, while BLUE assumes all the relative measurements are linear. Fourth, there are mobile nodes, i.e. firefighters, in the breadcrumb system. However, BLUE only considers static RMG.

To address the above issues, we describe a novel method based on an electrical analogy. It has a lower computation complexity, follows an incremental computation scheme, does not require all the relative measurements to be linear, and supports mobile nodes.

B. Incremental Estimation on Generalized Electrical Network

Rescue tasks may last a few hours and produce a large amount of measurements. Therefore, the number of measurements m will be much larger than the number of nodes n. To reduce the computational complexity and allow nodes joining, leaving and moving in the network, we use a novel computation scheme that analogizes the graph G into a circuit and utilizes electrical laws to compute $\hat{\mathbf{x}}_b$ and $\mathbf{\Sigma}$ incrementally.

It has been shown in [25] that a relative measurement graph $G = (V, E, F)$ is analogous to a generalized electrical network (GEN) $\mathcal{G} = (\mathcal{V}, \mathcal{E}, \mathcal{F})$, where $\mathcal{V}$ is the node set the same as in G, $\mathcal{E}$ is the edge set the same as in G, and $\mathcal{F} : \mathcal{E} \to \mathbf{R}$ is an edge function that assigns each edge e_k a matrix valued resistance $\mathbf{R}_k$ which is numerically equal to the measurement error covariance matrix $\mathbf{P}_k$ in the graph G.

The proof of the analogy between a RMG and a GEN can be found in [27]. Below we briefly explain the underlying idea. In BLUE, the estimate $\hat{\mathbf{x}}_i$ is a linear combination of all related measurements, i.e., $\hat{\mathbf{x}}_i = \Sigma_k \mathbf{J}_{ik}\mathbf{z}_k$, where $\mathbf{J}_{ik} \in \mathbb{R}^{3\times3}$ is a weight matrix. As a whole, BLUE minimizes $trace(cov((\mathbf{x} - \hat{\mathbf{x}}))) = trace(\Sigma_k \mathbf{J}_k \mathbf{P}_k \mathbf{J}_k^T)$. On the other hand, the Thomson's Principle [27] in multidimensional situation states that if flow $\mathcal{J}_k$ (any function of an edge) of a graph satisfy Kirchhoff's Laws, the flow uniquely minimizes the graph's energy dissipation, i.e., $trace(\Sigma_k \mathcal{J}_k \mathbf{R}_k \mathcal{J}_k^T)$. Since BLUE gives the result of minimum energy dissipation, the Kirchhoff's Laws holds in graph G. Therefore, RMG is analogous to GEN, where $\mathbf{P}_k$ is analogous to a general resistance $\mathbf{R}_k$, and weight matrix $\mathbf{J}_k$ is analogous to a generalized current.

The Kirchhoff's Current Law holds in the GEN. A generalized current $\mathbf{J}$ is defined as a 3×3 matrix associated with an edge with certain direction. For each node in $\mathcal{V}$, the net generalized current flowing out or into that node is $\mathbf{0}$.

The Kirchhoff's Voltage Law holds in the GEN as well. A generalized voltage potential difference $\mathbf{U}_{ij}$ between Node i and Node j is defined as a 3×3 matrix $\mathbf{U}_{ij} = \mathbf{R}_{ij} \times \mathbf{J}_{ij}$. For any loop in the $\mathcal{G}$, the sum of the generalized voltage potential difference in the clockwise or the counterclockwise direction is $\mathbf{0}$. If there are currents or voltages imposed to the GEN, each node is associated with a voltage potential. The anchor nodes are considered being connected to the ground without a resistance. For example, the location of the base station is assumed to be known without uncertainty, and thus its voltage potential is $\mathbf{0}$.

Fig. 5 shows the GEN analogy of the RMG example in Fig. 4. The resistances are numerically equal to the corresponding measurement error covariance matrix of the the edges. The Kirchhoff's Current and Voltage Laws are also illustrated in the figure.

Let $\mathbf{\Sigma}_{ii}$ denote Node i's estimation covariance matrix, i.e., the ith diagonal block element of covariance matrix $\mathbf{\Sigma}$. $\mathbf{\Sigma}_{ii}$ is numerically equal to the effective resistance $\mathbf{R}_i^{eff}$

between Node i and the ground in $\mathcal{G}$ [25]. To calculate $\mathbf{\Sigma}_{ii}$, we impose an identity generalized current $\mathbf{I}$ to Node i. Then Node i's voltage potential $\mathbf{U}_{ii}$ is numerically equal to $\mathbf{R}_i^{\mathit{eff}}$

$$\mathbf{U}_{ii} = \mathbf{R}_i^{\mathit{eff}} \times \mathbf{I} = \mathbf{\Sigma}_{ii}$$

Let's define the GEN $\mathcal{G}$ imposed by an identity current $\mathbf{I}$ on Node i as *Node i's Identity Current Graph*, denoted as $\mathcal{G}^i$. Let $\mathbf{U}_{jj}^{(i)}$ represent the voltage potential of Node j in $\mathcal{G}^i$. Let $\mathbf{\Phi_i} = [\mathbf{U}_{11}^{(i)T}, \mathbf{U}_{22}^{(i)T}, \cdots, \mathbf{U}_{n_b n_b}^{(i)T}]^T$ denote the n_b voltage potential variables in $\mathcal{G}^i$. Then with Kirchhoff's Current Law, the current balance equation for each node can be written as

$$\mathbf{L\Phi_i} = \mathbf{H}_i \tag{6}$$

where $\mathbf{H}_i = [\mathbf{0}, \mathbf{0}, \cdots, \mathbf{I}, \cdots, \mathbf{0}]^T \in \mathbb{R}^{3n_b \times 3}$, $\mathbf{0}$ is the 3×3 zero matrix and $\mathbf{I}$ is the 3×3 identity matrix. $\mathbf{L} \in \mathbb{R}^{3n_b \times 3n_b}, (i, j \in \{1, 2, \cdots, n_b\})$ and

$$\mathbf{L}_{ij} = \begin{cases} \sum\limits_{l \in \mathcal{V}} \mathbf{P}_{il}^{-1} (\text{or } \mathbf{P}_{li}^{-1}) & \text{if } i = j \text{ and } e_{li} \in \mathcal{E} \\ -\sum\limits_{i,j \in \mathcal{V}} \mathbf{P}_{ij}^{-1} (\text{or } \mathbf{P}_{ji}^{-1}) & \text{if } i \neq j \text{ and } e_{ij} \in \mathcal{E} \\ \mathbf{0} & \text{if } e_{ij} \notin \mathcal{E}. \end{cases} \tag{7}$$

Given that $\mathcal{L} = \mathcal{A}_b \mathcal{P}^{-1} \mathcal{A}_b^T$ and $\Sigma = \mathcal{L}^{-1}$, it is not hard to show that $\mathbf{L}$ is equal to $\mathcal{L}$ in (4).

In (6), only one identity current graph is considered. If all the identity current graphs are considered together, i.e., $\mathcal{G}^i$ for $i = 1, 2, \cdots, n_b$, then we have

$$\mathbf{L\Phi} = \mathbf{H} \tag{8}$$

where $\mathbf{\Phi} = [\mathbf{\Phi}_1, \mathbf{\Phi}_2, \cdots, \mathbf{\Phi}_{n_b}]$ is the voltage potential variable matrix and $\mathbf{H} = [\mathbf{H}_1, \mathbf{H}_2, \cdots, \mathbf{H}_{n_b}] = \mathbf{I} \in \mathbb{R}^{3n_b \times 3n_b}$. The solution of (8) is

$$\mathbf{\Phi} = \mathbf{L}^{-1} = \mathbf{\Sigma}$$

Considering the definition of $\mathbf{U}$, it can be seen that the covariance matrix $\mathbf{\Sigma}_{ij}$ between Node i and Node j is numerically equal to $\mathbf{U}_{ij}$ of Node i in Node j's $\mathcal{G}^j$. Since $\mathbf{\Sigma}$ is a symmetric matrix, it is also equal to the voltage potential $\mathbf{U}_{ji}$ of Node j in Node i's $\mathcal{G}^i$. Moreover, $\mathbf{b} = [\mathbf{b}_1^T, \cdots, \mathbf{b}_{n_b}^T]^T$ in (4) can be built directly as follows

$$\mathbf{b}_i = \sum_{e_{ij} \in \mathcal{E}} \mathbf{P}_{ij}^{-1} [\zeta_{ij} + \mathbf{c}_j], \tag{9}$$

$$\mathbf{c}_j = \begin{cases} \mathbf{x}_j & \text{if Node } j \text{ is an anchor node} \\ \mathbf{0} \in \mathbb{R}^{3 \times 1} & \text{otherwise} \end{cases} \tag{10}$$

By using (4) and (5), the node position estimations and the corresponding error covariance matrix can be derived.

The advantages of the analogy method are threefold. First, comparing with the BLUE method, the analogy method reduces computational complexity for constructing the matrix $\mathbf{L}$ from $O(mn^2)$ to $O(m)$, and the matrix $\mathbf{b}$ from $O(nm)$ to $O(m)$. After building the matrices $\mathbf{b}$ and $\mathbf{L}$, the computational complexity for $\hat{\mathbf{x}}_b$ is $O(n^2)$, and the complexity for $\mathbf{\Sigma}$ is $O(n^3)$ since the main complexity comes from the matrix inversion $\mathcal{L}^{-1}$. Second, it maps the localization problem to a circuit's Kirchhoff's matrix calculation problem. This not only makes the localization problem more intuitive, but also brings all the laws from circuit field to the localization field. Finally, since the Kirchhoff's matrix explicitly reflects a network's topology, when the topology changes (node joining/leaving, or measurements generated), only the corresponding elements of the Kirchhoff matrix are affected. This incremental computation scheme perfectly fits with the breadcrumb system which has many dynamic changes.

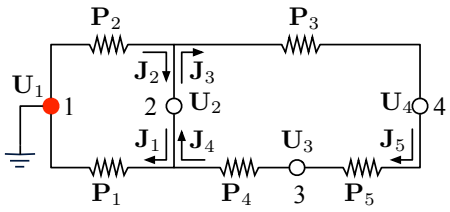

Figure 5. The GEN analogy of the RMG example. For Node 2, the Kirchhoff's Current Law holds: $\mathbf{P}_1^{-1}(\mathbf{U}_1 - \mathbf{U}_2) + \mathbf{P}_2^{-1}(\mathbf{U}_2 - \mathbf{U}_1) + \mathbf{P}_3^{-1}(\mathbf{U}_4 - \mathbf{U}_2) + \mathbf{P}_4^{-1}(\mathbf{U}_2 - \mathbf{U}_3) = \mathbf{0}$. And for the right side loop of Node 2, 3 and 4, the Kirchhoff's Voltage Law holds: $\mathbf{P}_3\mathbf{J}_3 + \mathbf{P}_4\mathbf{J}_4 + \mathbf{P}_5\mathbf{J}_5 = \mathbf{0}$.

C. Operations on GEN

In the breadcrumb network, there are many dynamic changes, including new measurements being generated, new nodes joining the network, and existing nodes leaving the network. To avoid re-computing all the values when changes happen, we define three operations on the GEN, so that we only need to modify the equations for the involved nodes.

1. AddMeasurement. When a new measurement ζ_{ij} is generated, if Node i and Node j are both non-anchor nodes, according to Kirchhoff's Current Law or (7), updates are done using the following equations

$$\begin{bmatrix} \mathbf{L}_{ii} & \mathbf{L}_{ij} \\ \mathbf{L}_{ji} & \mathbf{L}_{jj} \end{bmatrix} = \begin{bmatrix} \mathbf{L}_{ii} & \mathbf{L}_{ij} \\ \mathbf{L}_{ji} & \mathbf{L}_{jj} \end{bmatrix} + \begin{bmatrix} \mathbf{P}_{ij}^{-1} & -\mathbf{P}_{ij}^{-1} \\ -\mathbf{P}_{ji}^{-1} & \mathbf{P}_{ji}^{-1} \end{bmatrix}$$
$$\begin{bmatrix} \mathbf{b}_i \\ \mathbf{b}_j \end{bmatrix} = \begin{bmatrix} \mathbf{b}_i \\ \mathbf{b}_j \end{bmatrix} + \begin{bmatrix} \mathbf{P}_{ij}^{-1}\zeta_{ij} \\ \mathbf{P}_{ji}^{-1}\zeta_{ji} \end{bmatrix} \tag{11}$$

If Node u is an anchor node, update

$$\begin{aligned} \mathbf{L}_{jj} &= \mathbf{L}_{jj} + \mathbf{P}_{ji}^{-1} \\ \mathbf{b}_j &= \mathbf{b}_j + \mathbf{P}_{ji}^{-1}(\zeta_{ji} + \mathbf{x}_i) \end{aligned} \tag{12}$$

When a node joins or leaves the network, it only affects the node and its neighbors. Next we define an operation to handle this kind of event.

2. AddNode. If a node joins the network with some measurements to some already existing nodes, use the following

operation to first allocate new rows and columns to $\mathbf{L}$ and $\mathbf{b}$ for the new node

$$\mathbf{L} = \begin{bmatrix} \mathbf{L} & \mathbf{0} \\ \mathbf{0} & \mathbf{0} \end{bmatrix}, \mathbf{b} = \begin{bmatrix} \mathbf{b} \\ \mathbf{0} \end{bmatrix} \tag{13}$$

Then we apply the *AddMeasurement* operation on each newly introduced measurement.

3. DeleteNode. If a node leaves the network, its information need to be safely forgotten. This process is called *marginalization*. From the perspective of probability, it is $P(A) = \int f(A, B)dB$ where A is the variable to keep and B is the variable to drop. If we have

$$\hat{\mathbf{x}}_b = \begin{bmatrix} \hat{\mathbf{x}}_1 \\ \hat{\mathbf{x}}_\pi \end{bmatrix}, \mathbf{\Sigma} = \begin{bmatrix} \mathbf{\Sigma}_{11} & \mathbf{\Sigma}_{1\pi} \\ \mathbf{\Sigma}_{\pi 1} & \mathbf{\Sigma}_{\pi\pi} \end{bmatrix} \tag{14}$$

where Node 1 is the node to be deleted and the subscript π is a block index that refers to all the other indexes (except 1). Then the delete operation on $\hat{\mathbf{x}}_b$ and $\mathbf{\Sigma}$ is to simply delete the corresponding rows and columns

$$\hat{\mathbf{x}}_b = \hat{\mathbf{x}}_\pi, \mathbf{\Sigma} = \mathbf{\Sigma}_{\pi\pi} \tag{15}$$

For $\mathbf{L}$ and $\mathbf{b}$, before the deletion

$$\mathbf{L} = \begin{bmatrix} \mathbf{L}_{11} & \mathbf{L}_{1\pi} \\ \mathbf{L}_{\pi 1} & \mathbf{L}_{\pi\pi} \end{bmatrix}, \mathbf{b} = \begin{bmatrix} \mathbf{b}_1 \\ \mathbf{b}_\pi \end{bmatrix} \tag{16}$$

According to the relation between $\mathbf{L}$ and $\mathbf{\Sigma}$ specified in (5), and the relation between $\mathbf{b}$ and $\hat{\mathbf{x}}_b$ given by (4), the delete operation is

$$\begin{aligned} \mathbf{L} =& \mathbf{L}_{\pi\pi} - \mathbf{L}_{\pi 1}\mathbf{L}_{11}^{-1}\mathbf{L}_{\pi 1}^T \\ \mathbf{b} =& \mathbf{b}_\pi - \mathbf{L}_{\pi 1}\mathbf{L}_{11}^{-1}\mathbf{b}_1 \end{aligned} \tag{17}$$

D. Non-linear Measurements

In the breadcrumb system, the relative measurements output by PDR is linear, while the ranging measurements based on two nodes' RSSI are non-linear. Next we extend the GEN method to the non-linear case.

The relative measurement (1) can be expanded by Taylor series at $\hat{\mathbf{x}}_{ij}$ to the first order as $\tilde{\mathbf{z}}_{ij} = h(\hat{\mathbf{x}}_{ij}) + \mathbf{H}(\mathbf{x}_{ij} - \hat{\mathbf{x}}_{ij}) + \epsilon_{ij}$, where $\tilde{\mathbf{z}}_{ij}$ is the linear approximation for $\mathbf{z}_{ij}$, and $\mathbf{H}$ is the derivative of measurement function $h(\cdot)$.The three operations are modified as follows.

1. AddMeasurement+. According to the information filter [28]–[30] , the AddMeasurement operation, i.e., (11) is extended to

$$\mathbf{L}_\mathbf{z} = \mathbf{L}_\mathbf{z} + \mathbf{H}^T\mathbf{P}_\mathbf{z}^{-1}\mathbf{H} \tag{18}$$

$$\mathbf{b}_\mathbf{z} = \mathbf{b}_\mathbf{z} + \mathbf{H}^T\mathbf{P}_\mathbf{z}^{-1}(\mathbf{z} - h(\hat{\mathbf{x}}) + \mathbf{H}\hat{\mathbf{x}}) \tag{19}$$

where $\mathbf{L}_\mathbf{z}$ represents the sub-matrix of $\mathbf{L}$ that contains the elements of involved nodes. This is similar for the vector $\mathbf{b}_z$. $\mathbf{P}_\mathbf{z}$ is the error covariance matrix of involved measurement errors. $\hat{\mathbf{x}}$ is the latest position estimate and the point that the derivative function is evaluated on. For example, for a relative ranging measurement between Node i and Node j

$$\mathbf{L}_\mathbf{z} = \begin{bmatrix} \mathbf{L}_{ii} & \mathbf{L}_{ij} \\ \mathbf{L}_{ji} & \mathbf{L}_{jj} \end{bmatrix}, \mathbf{H} = \begin{bmatrix} \mathbf{h}_{ij} \\ -\mathbf{h}_{ij} \end{bmatrix}$$

where

$$\mathbf{h}_{ij} = \frac{(\hat{\mathbf{x}}_i - \hat{\mathbf{x}}_j)^T}{\|\hat{\mathbf{x}}_i - \hat{\mathbf{x}}_j\| + \epsilon_{ij}}$$

According to (7) and (9), we can also build $\mathbf{L}$ and $\mathbf{b}$ directly

$$\mathbf{L}_{ij} = \begin{cases} \sum\limits_{l\in\mathcal{V}} \mathbf{h}_{il}^T\mathbf{P}_{il}^{-1}\mathbf{h}_{il} & \text{if } i = j \text{ and } e_{li} \in \mathcal{E} \\ -\sum\limits_{i,j\in\mathcal{V}} \mathbf{h}_{ij}^T\mathbf{P}_{ij}^{-1}\mathbf{h}_{ij} & \text{if } i \neq j \text{ and } e_{ij} \in \mathcal{E} \\ \mathbf{0} & \text{if } e_{ij} \notin \mathcal{E}. \end{cases} \tag{20}$$

$$\mathbf{b}_i = \sum_{e_{ij}\in\mathcal{E}} \mathbf{h}_{ij}^T\mathbf{P}_{ij}^{-1}(\mathbf{z}_{ij} - h([\hat{\mathbf{x}}_i^T, \hat{\mathbf{x}}_j^T]^T) + \mathbf{H}[\hat{\mathbf{x}}_i^T, \hat{\mathbf{x}}_j^T]^T) \tag{21}$$

For the relative ranging measurements, $h([\hat{\mathbf{x}}_i^T, \hat{\mathbf{x}}_j^T]^T) = \|\hat{\mathbf{x}}_i - \hat{\mathbf{x}}_j\|$. For relative position measurements, $h([\hat{\mathbf{x}}_i^T, \hat{\mathbf{x}}_j^T]^T) = \hat{\mathbf{x}}_i - \hat{\mathbf{x}}_j$ and $\mathbf{h}_{ij} = \mathbf{I} \in \mathbb{R}^{2\times 2}$. In the second case (linear measurements), (20) and (21) degrade to (7) and (9).

2. AddNode+. In the non-linear case, when a node joins the network with some measurements, we still first add new rows and columns like (13). But then the AddMeasurement+ operation is used on each new measurements, instead of AddMeasurement.

3. DeleteNode+. The DeleteNode+ operation remains the same as DeleteNode. Since we still need to delete the corresponding rows and columns, i.e., (15) holds, and after linearization (4) and (5) hold as well.

E. Mobile Nodes

To take the mobility of firefighters into consideration, we need to extend the relative measurement graph model. An *extended relative measurement graph (ERMG)* is defined based on relative measurement graph (RMG). The difference is that a vertex in an ERMG is a *state* which is identified by the node ID and the timestamp. This means the same firefighter is treated as different vertices at different time stamps in the ERMG. Then the movement of a firefighter would be seen as adding and deleting states successively through the three operations described in Section IV-D. Since breadcrumbs are stationary once deployed, they do not need to be treated as different nodes at different times. So they are identified by their node IDs. An example is shown in Fig. 6.

At timestamp 1, there are 3 breadcrumbs in the network: Node 1, Node 2 and Node 3. In Fig. 6a, at timestamp 2, a firefighter Node 4.2 joins the network and produces new measurement $\mathbf{z}_5$ and $\mathbf{z}_6$ with Node 1 and Node 3 respectively. The AddNode+ measurement is used to update the ERMG to reflect these changes. In Fig. 6b, the firefighter moves to a new position and the state changes from Node 4.2

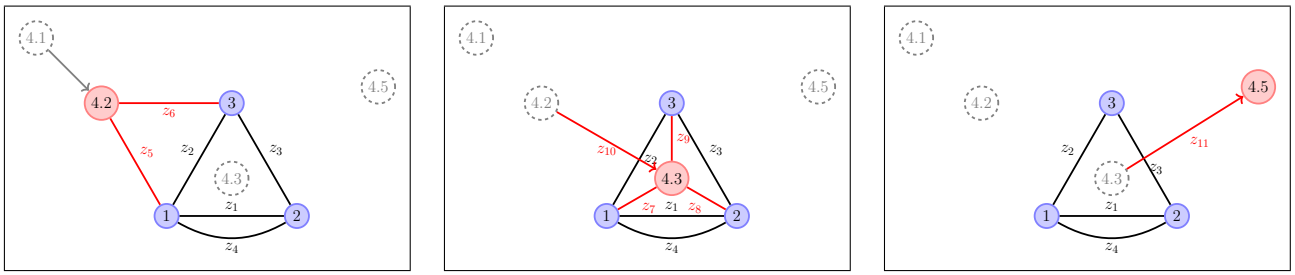

(a) A firefighter (Node 4) joins in the ERMG at timestamp 2.

(b) The firefighter moves in the ERMG from timestamp 2 to timestamp 3.

(c) The firefighter continue moves and finally leaves the ERMG at timestamp 5.

Figure 6. An ERMG example.

to Node 4.3. New measurements $\mathbf{z}_7$, $\mathbf{z}_8$ and $\mathbf{z}_9$ are generated. The relative position measurement $\mathbf{z}_{10}$ measured by the PDR unit connects the old state Node 4.2 with the new state 4.3. We first apply the AddNode+ operation to add the new state 4.3. Then the old state Node 4.2 is deleted through the DeleteNode+. In Fig. 6c, the firefighter leaves the network. The delete operation is used to to delete the Node from the network. In each moment, once $\mathbf{L}$ and $\mathbf{b}$ are updated, the position estimation $\hat{\mathbf{x}}_b$ and the covariance matrix $\mathbf{\Sigma}$ can be calculated according to (4) and (5).

F. The Discussion and Analysis of the Breadcrumb Localization System

The GEN method is deduced based on the electrical laws and gives the same result (estimate and covariance matrix) as BLUE. BLUE and the GEN method are equivalent mathematically. In fact, the incremental computation scheme can be derived by analyzing the structure of matrices in (4) as well. But the circuit analogy provides more insights of the decomposition operations. In GEN, the Kirchhoff's Laws vividly reveal the relationship of measurements and covariance matrices which is not so intuitive to see through BLUE. Based on the meaning of $\mathbf{L}$ and $\mathbf{b}$, we can build three operations to add measurements, add nodes and delete nodes more easily.

The beauty of the breadcrumb localization system is fourfold. First, it does not rely on any pre-installed infrastructure. The breadcrumbs are deployed in a "just-in-time" manner, and the PDR unit works as a self contained module. Second, the system solves not only the localization problem, but also the communication problem. The location information is now able to reach both the base station and all the team members (breadcrumbs/firefighters) in a more confident way. Third, in the system, all nodes are highly correlated. The benefit of this is that any new positioning information which only involves limited number of nodes can be propagated to the whole network. This helps the localization to be converged quickly. Fourth, the breadcrumbs on the ground are fixed, which means the trace of their error covariance matrix, representing the position mean square error, can only be decreased as more and more measurements are brought in by firefighters or generated by themselves. Therefore, the breadcrumbs can work as landmarks to "calibrate" firefighters' position estimation when they pass by.

In practice, the world is not clean. There are accurate measurements and non-accurate measurements. The third and the fourth properties in the above can enlarge the effect of both accurate measurements and non-accurate measurements. Therefore, we should differentiate the non-accurate measurements from accurate measurements, and then either drop them or lessen their effect. For example, a firefighter has physical limitation (e.g. the maximum speed is less than 5m/s). If any measurement breaks this limitation, we can simply drop it. Another example is that sometimes a measurement is generated with lots of noise. Then we should associate this measurement with an error covariance matrix having a large trace value, which will weaken its impact to the whole system.

Beside the good features, we are also interested in the error bound of the breadcrumb localization system. By embedding the ERMG of a breadcrumb network into a infinite generalized electrical lattice, we can determine the bound of the estimation error [24]. The scaling laws for the covariance matrix of the estimation error for an ERMG are listed in Table IV-F. The error bound of covariance matrix of the estimation error $\mathbf{\Sigma}$ for an ERMG of a breadcrumb network. d_{io} denotes the Euclidean distance between Node i to reference node o. The covariance matrices of relative measurement errors satisfy $\|\mathbf{P}_{min}\| \leq \|\mathbf{P}\| \leq \|\mathbf{P}_{max}\|$. $\alpha_j, \beta_j, (j = 1, 2, 3)$ are constants determined by the structure of the ERMG. It can be seen that in a one-dimensional lattice, the covariance matrix of estimation error (effective resistance) grows linearly with the distance between nodes. In a three-dimensional lattice, the effective resistance is bound by constants.

Dim.	Bound of $\mathbf{\Sigma}_i$
$\mathbb{R}^1$	$\alpha_1 d_{io}\|\mathbf{P}_{min}\| \leq \|\mathbf{\Sigma}_i\| \leq \beta_1 d_{io}\|\mathbf{P}_{max}\|$
$\mathbb{R}^2$	$\alpha_2 \log(d_{io})\|\mathbf{P}_{min}\| \leq \|\mathbf{\Sigma}_i\| \leq \beta_2 \log(d_{io})\|\mathbf{P}_{max}\|$
$\mathbb{R}^3$	$\alpha_3\|\mathbf{P}_{min}\| \leq \|\mathbf{\Sigma}_i\| \leq \beta_3\|\mathbf{P}_{max}\|$

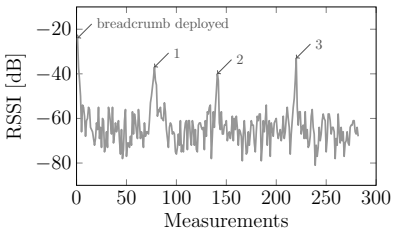

Figure 7. The points of encounter.

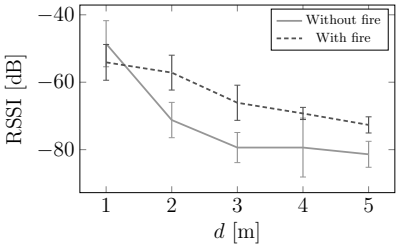

Figure 8. Impact of smoke and fire on communication links.

In practice, the RMG of most wireless sensor networks, such as the breadcrumb network, can be embedded in a two or three dimensional lattice, which means the covariance matrix of estimation error would grow as the logarithm of graphical distance. Considering that the accumulated error of a PDR module grows linearly with the total travel distance (which is usually longer than the graphical distance), after a certain point, the firefighter would obtain better location estimate by utilizing the interactions with breadcrumbs than merely using the PDR module. However, the constants also affect the performance of the system. In Section V, we conduct several experiments to evaluate the proposed solution.

V. Evaluation

We have built a prototype of our system to localize firefighters in harsh indoor environments. The system hardware is shown in Fig. 2 which includes a breadcrumb dispenser, multiple breadcrumbs, a base station, and a PDR unit. The PDR unit is placed in the boot of the user. Fig. 3 shows a firefighter wearing a full set of equipment. The communication is all based on 2.4GHz chips and the Zigbee protocol. Please refer to [10] for using the Zigbee stack and 2.4 GHz based hardware instead of lower frequencies like 900 MHz. Floor plans are not required by our system.

In this section we validate our system with several experiments. Section V-A presents the results of localization and the interactions between firefighters and breadcrumbs. Section V-B reports an in-field experiment conducted in a simulated on-fire industrial building to evaluate the overall system and study the impact of fire and smoke. Section V-C summaries feedback from professional firefighters and lessons learned from the experiments.

A. Interactions and Localization Accuracy

Experimental Setup. A series of experiments are conducted on the 4th floor of an office building. Fig. 9a displays the floor map. We set the right up-most corner as the starting of the experimental trace. The base station is placed at this point. The circular trajectory is also illustrated in the figure and has a total length of 400 (100×4) meters. Six breadcrumbs are automatically deployed as a user walks anti-clockwise along this trace and returns to the starting point. Then this user continues walking along this trace three more times. The initial positions of breadcrumbs are calculated from the PDR component attached to the shoes of the users. The user's device interacts with the breadcrumbs after they are deployed. The positions of the user and breadcrumbs are recorded throughout the experiment.

Goals. The goal of these experiments is to study the interactions between firefighters and breadcrumbs, as well as validate the benefits of utilizing them to assist localization. Interactions include encounter events and relative measurements between firefighters and breadcrumbs. We also compare the localization performance of our proposed method with PDR-based method.

Results. Fig. 7 shows an example of RSSI values between the user and one breadcrumb during the experiment. We can observe three peaks of the RSSI value. When an encounter (a user passes by a breadcrumb) happens, the RSSI value is higher than $-40dB$ which implies the distance between the user and the breadcrumb is about or less than 1 meter. In the following experiments, we define these points as the ground truth of encounters between the user and breadcrumbs. We adopt the approach used in [31], in which the RSSI values are analyzed and points with local optimum are considered as the positions where encounters occur.

Fig. 9b shows the estimated trajectory when the PDR component utilizes the breadcrumb system for communication purposes only, but not for localization assistance. It is clear that the trajectory displayed at the command center completely lost the user (firefighter) and the location error at the end of the trace is more than 35 meters. Using PDR without the help from the breadcrumb system may result in huge cumulative error.

Fig. 9c displays the estimated trajectory using our approach. The PDR module is the same one used in 9b and the data is collected in the same experiment. We observe that the shape of the trajectory is much better preserved compared with the PDR approach. This is important for incident commanders to issue correct orders to firefighters when emergencies happen.

Localization accuracy is the main evaluation metric in our system. We describe the average results of eight traces and one representative trace of a user, in order to show how our approach helps improve localization accuracy. Fig. 12

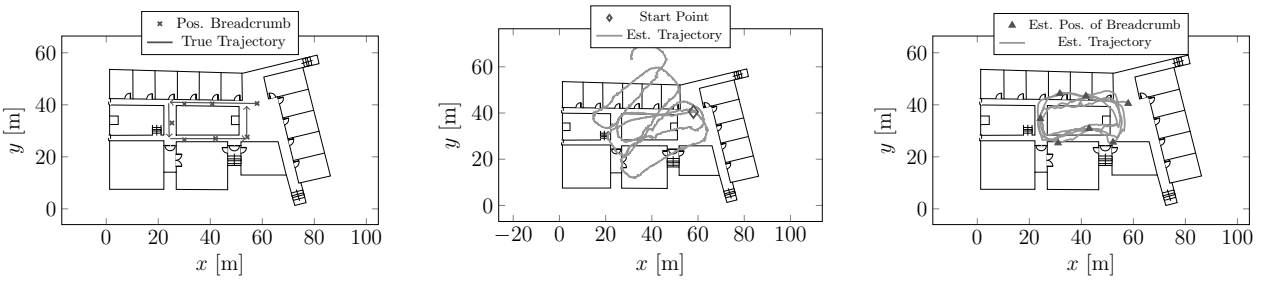

(a) Laboratory experiment floor map. (b) Estimated trace using the PDR method (c) Estimated trace using the proposed method.

Figure 9. Estimated trace during the 400 meter experiment.

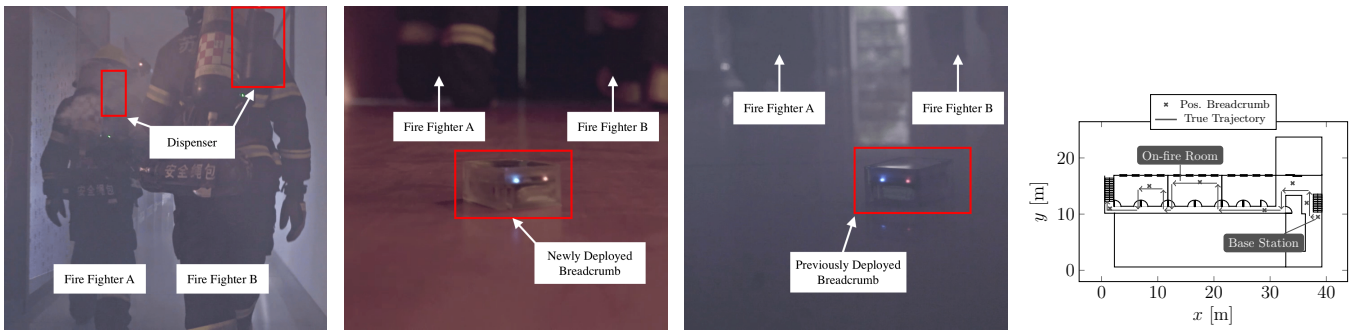

(a) Firefighters Enter the Building. (b) Deploy a Breadcrumb. (c) Encounter and Pass by a Breadcrumb. (d) Field experiment floor map.

Figure 10. Field experiment.

shows the location error of the user as he encounters the breadcrumbs during the representative trace. First, we observe that the location error increases to 7.3 meters after the first round. The location error is already 5.4 meters when the user deploys the second breadcrumb. It is mainly because PDR is subject to cumulative errors. Second, the location error oscillates for the remaining rounds, which implies that breadcrumbs provide considerable help to bound the location error of the user. The average error along this 400 meter long trace is 5.5 meters, and the maximum location error is 10.4 meters, which indicates that our approach leads to the location error of 2.5% of the total distance. This is quite a promising result and acceptable in firefighting applications. Fig. 13 shows the location error of the user in all eight traces. We find the same trend in all cases, the average of average location error is 5.6 meters, and the average of maximum location error is 10.9 meters, which implies a promising 1.4% and 2.7% error for the total distance.

We also study the convergence of the proposed solution. Fig. 11 draws a representative example of the location error of a breadcrumb with varying number of measurements. We observe that the estimation error increase slightly at the beginning. This is reasonable since the total travel distance is still short at the beginning and the PDR module is more accurate than the relative range measurements for the moment, i.e. $\mathbf{P}_{PDR} \leq \mathbf{P}_{RSSI}$. Therefore, with the generation of more relative range measurements, the location error may raise slightly for this unstable stage. With the increase of the travel distance, more breadcrumbs are deployed, the network dimension is changed from $\mathbb{R}$ to $\mathbb{R}^2$, so a significant error reduction is observed between 750 to 1,250 measurements. The best location accuracy is between 1,000 to 1,500 measurements. The result agrees with the RMG convergence property analyzed in [25] which states that after a certain point, considering more measurements will only marginally improve the quality of the estimate. Note that both relative range measurements and relative position measurements are included. The former are obtained by analyzing the RSSI value of communication packets. The latter are the PDR readings reported by the PDR units periodically. Therefore, it is easy to collect thousands of measurements in practice.

B. *In-field Experiments*

Experimental Setup. We also perform experiments on the 3rd floor of a firefighting building in cooperation with Suzhou Fire Department. Fig. 10d displays the floor map. To simulate a real scene, an actual fire is setup to produce smoke, flames and heat. A smoke bomb is also used to produce extra smoke so that the smoke volume is similar to a real situation. The base station is located close to the

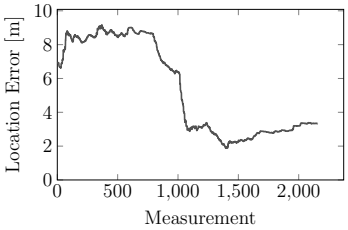

Figure 11. Breadcrumb location error.

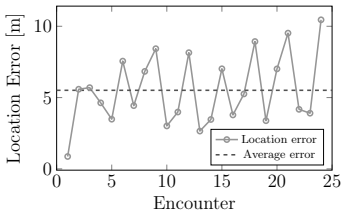

Figure 12. Location error of the user along the trace.

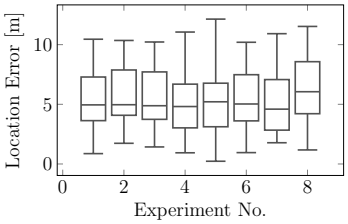

Figure 13. Localization accuracy in all cases.

right entrance. Two firefighters are equipped with our system and behave as usual under normal rescue tasks (shown in Fig. 10a), including searching and fire extinguishing. Breadcrumbs are deployed automatically along their trajectory (depicted in Figure 10c). We also measure the impact of heat and smoke on RSSI by placing two breadcrumbs at both sides of fire and assess their communication quality. To better present the results, we decrease the transmission power in this experiment. The RSSI between two breadcrumbs from 1 meter to 5 meters are recorded.

Goal. The goal of the in-field experiment is to validate the system robustness in real-world firefighting scenes and demonstrate that our proposed indoor localization system works in complicated environments. We evaluate the environment factors such as heat and smoke on the system, from the RSSI values.

Results. As one of the most important factors in a firefighting application, the impact of fire is evaluated. As shown in Fig. 8, the solid line is obtained according to the RSSI-ranging model in the same building without fire. The dashed line is the RSSI curve with fire on the scene. It can be seen that fire (presumably heat) affects RSSI significantly. The accuracy of ranging calculated from RSSI drops as the distance becomes larger. Together with the result of the encounter experiment (shown in Fig. 7), it can be seen that relative range measurements within 1.5 meter are relatively accurate. Encounter events are still easy to detect. Moreover, the result implies that RSSI may be a good indicator to monitor the changes in the network. For example, if the RSSI between a pair of breadcrumbs varies suddenly, it may indicate the movement of breadcrumbs or change of surrounding environments. By analyzing the RSSI changes between breadcrumbs, we may infer the precise reason and claim that this region has already been on fire and is no longer safe for firefighters to pass through.

C. Lessons Learned

We also collect valuable feedback from firefighters in the in-field experiment. The motivation and requirement analysis of our work are recognized by the firefighters. They especially appreciate the automatic and infrastructure-free design. However, they also proposed several issues to consider.

The first problem is caused by water. Although the breadcrumbs are designed to be waterproof (IP67), we did not expect the problem caused by plashes. The firefighters report that in some cases there would be as deep as $30cm$ to $40cm$ water accumulated on the ground. This could be problematic since the current breadcrumb system uses the Zigbee protocol whose frequency is 2.4GHz and radio wave at 2.4GHz can be absorbed by water easily. They also report that plashes usually are on the ground floor and the basement. Using foam to replace water for firefighting is gradually becoming a common practice so its impact needs to be studied.

Firefighters also expressed concern on accidentally kicking breadcrumbs. However, when the visibility is low due to smoke and low ambient light, firefighters will use a so-called "trail step" and walk very slowly. In such cases, breadcrumbs may be stepped on, but less possible to be kicked away for a long distance. According to the test, the displacement is usually within 1 to 2 meters if the breadcrumb is accidentally kicked. Even if a breadcrumb moved to a new position, with the generation of new measurements, the localization error can then be reduced subsequently.

VI. Conclusion

This paper presents the design, implementation, and evaluation of an automatic and accurate localization system, motivated by the important needs on firefighter safety. All previous work failed to provide an automatic, accurate, and reliable solution to localize firefighters in harsh environments. This paper proposes a novel system to achieve this goal, by combining pedestrian dead reckoning with a recently emerging breadcrumb system. We described the details of a novel collaborative localization algorithm that leverages the interaction between dispensers and breadcrumbs. We fully implemented this system, and compared our solution to pedestrian dead reckoning. Evaluation results show that our approach reduces the maximum firefighter location error and outperforms the alternative solution. In addition, on-field experiments by professional firefighters prove that our system is robust and functions well in complicated and harsh environments.

ACKNOWLEDGMENT

This work was partially funded by NSFC-61472384 as well as collaborative research program by the Fire Department of Ministry of Public Security in China.

REFERENCES

[1] "September 11 attacks," https://en.wikipedia.org/w/index.php?title=September_11_attacks&oldid=692920730.

[2] "Project 25." [Online]. Available: https://en.wikipedia.org/w/index.php?title=Project_25&oldid=682287192

[3] M. R. Souryal, J. Geissbuehler, L. E. Miller, and N. Moayeri, "Real-time deployment of multihop relays for range extension," in *Proceedings of the 5th international conference on Mobile systems, applications and services*. ACM, 2007, pp. 85–98.

[4] V. Amendolare, D. Cyganski, R. Duckworth, S. Makarov, J. Coyne, H. Daempfling, and B. Woodacre, "Wpi precision personnel locator system: Inertial navigation supplementation," in *Position, Location and Navigation Symposium, 2008 IEEE/ION*. IEEE, 2008, pp. 350–357.

[5] O. Woodman and R. Harle, "Pedestrian localisation for indoor environments," in *In Proceedings of the 10th international conference on Ubiquitous computing*. ACM, 2008, pp. 114–123.

[6] Y. Huang, W. He, K. Nahrstedt, and W. C. Lee, "Requirements and System Architecture Design Consideration for First Responder Systems," in *2007 IEEE Conference on Technologies for Homeland Security*, May 2007, pp. 39–44.

[7] T. Gdeke, J. Schmid, W. Stork, and K. D. Mller-Glaser, "Pedestrian dead reckoning for person localization in a wireless sensor network," *International Conference on Indoor Positioning and Indoor Navigation*, 2011.

[8] J. Schmid, T. Gdeke, W. Stork, and K. D. Mller-Glaser, "On the fusion of inertial data for signal strength localization," in *Positioning Navigation and Communication (WPNC), 2011 8th Workshop on*. IEEE, 2011.

[9] A. Correa, M. Barcelo, A. Morell, and J. L. Vicario, "Enhanced Inertial-Aided Indoor Tracking System for Wireless Sensor Networks: A Review," *IEEE Sensors Journal*, Sep. 2014.

[10] H. Liu, J. Li, Z. Xie, S. Lin, K. Whitehouse, J. A. Stankovic, and D. Siu, "Automatic and robust breadcrumb system deployment for indoor firefighter applications," in *Proceedings of the 8th international conference on Mobile systems, applications, and services - MobiSys '10*, 2010.

[11] K. Leung, T. Barfoot, and H. Liu, "An automatic, robust, and efficient multi-user breadcrumb system for emergency response applications," *Mobile Computing, IEEE Transactions on*, vol. 13, no. 4, pp. 723–736, 2014.

[12] H. Liu, P. Hui, Z. Xie, J. Li, D. Siu, G. Zhou, L. Huang, and J. A. Stankovic, "Providing reliable and real-time delivery in the presence of body shadowing in breadcrumb systems," *ACM Transactions on Embedded Computing Systems (TECS)*, vol. 13, no. 4, p. 94, 2014.

[13] S. Kumar, S. Gil, D. Katabi, and D. Rus, "Accurate Indoor Localization with Zero Start-up Cost," in *Proceedings of the 20th Annual International Conference on Mobile Computing and Networking*, ser. MobiCom '14. ACM, 2014.

[14] Z. Yang, Z. Wang, J. Zhang, C. Huang, and Q. Zhang, "Wearables Can Afford: Light-weight Indoor Positioning with Visible Light," in *Proceedings of the 13th Annual International Conference on Mobile Systems, Applications, and Services*, ser. MobiSys '15. ACM, 2015.

[15] Microsoft Research. Microsoft Indoor Localization Competition - IPSN 2015. [Online]. Available: http://research.microsoft.com/en-us/events/indoorloccompetition2015/

[16] Velodyne Acoustics Inc., "Datasheet of High Definition LiDAR HDL-32e," http://velodynelidar.com/docs/datasheet/97-0038_Rev%20D2_%20HDL-32E_datasheet_LowRes(web).pdf.

[17] H. Wang, S. Sen, A. Elgohary, M. Farid, M. Youssef, and R. R. Choudhury, "No need to war-drive: unsupervised indoor localization," in *Proceedings of the 10th international conference on Mobile systems, applications, and services*. ACM, 2012.

[18] H. Liu, A. Srinivasan, K. Whitehouse, J. Stankovic *et al.*, "Melange: Supporting heterogeneous QoS requirements in delay tolerant sensor networks," in *Networked Sensing Systems (INSS), 2010 Seventh International Conference on*. IEEE, 2010, pp. 93–96.

[19] E. Foxlin, "Pedestrian tracking with shoe-mounted inertial sensors," *IEEE Computer Graphics and Applications*, vol. 25, no. 6, pp. 38–46, 2005.

[20] J.-O. Nilsson, A. K. Gupta, and P. Hndel, "Foot-mounted inertial navigation made easy," in *International Conference on Indoor Positioning and Indoor Navigation*, 2014.

[21] Y. Huang, W. He, K. Nahrstedt, and W. C. Lee, "Incident Scene Mobility Analysis," in *2008 IEEE Conference on Technologies for Homeland Security*, May 2008, pp. 257–262.

[22] Y. Huang, W. He, K. Nahrstedt, and W. C. Lee, "CORPS: Event-driven mobility model for first responders in incident scene," in *MILCOM 2008 - 2008 IEEE Military Communications Conference*, Nov. 2008, pp. 1–7.

[23] Y. Huang, Y. Gao, and K. Nahrstedt, "Relay Placement for Reliable Base Station Connectivity in Polymorphous Networks," in *2010 7th Annual IEEE Communications Society Conference on Sensor, Mesh and Ad Hoc Communications and Networks (SECON)*, Jun. 2010, pp. 1–9.

[24] P. Barooah and J. Hespanha, "Estimation on graphs from relative measurements," *IEEE Control Systems*, vol. 27, no. 4, pp. 57–74, 2007.

[25] P. Barooah and J. Hespanha, "Estimation from relative measurements: Electrical analogy and large graphs," *IEEE Transactions on Signal Processing*, vol. 56, no. 6, pp. 2181–2193, 2008.

[26] J. M. Mendel, *Lessons in estimation theory for signal processing, communications, and control*. Pearson Education, 1995.

[27] P. G. Doyle and J. L. Snell, *Random Walks and Electric Networks*. Mathematical Association of America,, 1984.

[28] H. Mu, T. Bailey, P. Thompson, and H. Durrant-Whyte, "Decentralised Solutions to the Cooperative Multi-Platform Navigation Problem," *IEEE Transactions on Aerospace and Electronic Systems*, vol. 47, no. 2, pp. 1433–1449, Apr. 2011.

[29] Z. Xie, M. Hong, H. Liu, J. Li, K. Zhu, and J. Stankovic, "Quantitative uncertainty-based incremental localization and anchor selection in wireless sensor networks," in *Proceedings of the 14th ACM international conference on Modeling, analysis and simulation of wireless and mobile systems - MSWiM '11*, 2011.

[30] Z. Xie, "Collaborative localization using wireless sensor networks," Ph.D. dissertation, Univeristy of Virginia, 2016.

[31] G. Shen, Z. Chen, P. Zhang, T. Moscibroda, and Y. Zhang, "Walkie-markie: Indoor pathway mapping made easy," in *Proceedings of the 10th USENIX conference on Networked Systems Design and Implementation*. USENIX Association, 2013.